

Title	Ordering of island-like FePt crystallites with orientations
Author(s)	Bian, Bo; Sato, Kazuhisa; Hirotsu, Yoshihiko et al.
Citation	Applied Physics Letters. 1999, 75(23), p. 3686-3688
Version Type	VoR
URL	https://hdl.handle.net/11094/89389
rights	This article may be downloaded for personal use only. Any other use requires prior permission of the author and AIP Publishing. This article appeared in Bo Bian, Kazuhisa Sato, and Yoshihiko Hirotsu, "Ordering of island-like FePt crystallites with orientations", Appl. Phys. Lett. 75, 3686-3688 (1999) and may be found at https://doi.org/10.1063/1.125429 .
Note	

Osaka University Knowledge Archive : OUKA

<https://ir.library.osaka-u.ac.jp/>

Osaka University

Ordering of island-like FePt crystallites with orientations

Bo Bian,^{a)} Kazuhisa Sato, and Yoshihiko Hirotsu

The Institute of Scientific and Industrial Research, Osaka University, 8-1 Mihogaoka, Ibaraki, Osaka 567, Japan

Akihiro Makino

Central Laboratory, Alps Electric Company, Ltd., 1-3-5 Higashitakami, Nagaoka, Niigata 940, Japan

(Received 7 May 1999; accepted for publication 15 October 1999)

Thin films of oriented island-like crystallites of $L1_0$ FePt separated by amorphous (a -)Al₂O₃ were fabricated. The process took advantage of the overgrowth of α -Fe on Pt "seed" particles epitaxially grown on (100) NaCl and MgO substrates and the ordering reaction between Fe and Pt upon annealing at temperatures higher than 500 °C. The coercivities of the annealed (600 °C for 6 h) a -Al₂O₃/Fe(1 nm)/Pt (1.5 nm) films on both the NaCl (100) and MgO (100) substrates are higher than 3.3 kOe. Transmission electron microscopy observation showed that the film consisted of oriented $L1_0$ FePt island-like crystals with an average size of 12 nm and a separation of 4 nm. It was found that any one of the three $\langle 100 \rangle$ axes of the fcc Pt parent particles could act as the tetragonal c axis of the $L1_0$ FePt superstructure and all three-variant ordered crystalline domains of the tetragonal $L1_0$ phase could exist in the small 10-nm-size FePt crystallites. The high magnetic coercivity of the film, with well-separated FePt particles, can be attributed to the ordering ($L1_0$) as well as the oriented nature of the FePt crystallites. © 1999 American Institute of Physics.

[S0003-6951(99)03149-6]

The demand for higher-density magnetic storage media is one of the fundamental motivations for the investigation of granular magnetic materials.^{1,2} Generally, a higher storage density with lower noise is associated with a smaller magnetic grain size. However, the magnetic moment orientations of very small particles are easily perturbed by thermal agitation. Therefore, thermal stability is one of the key issues to be dealt with and an improvement in recording density is tied to obtaining an increase of magnetocrystalline anisotropy in tiny magnetic particles.^{3,4} Future-generation magnetic recording media are expected to have a coercivity of 3 kOe, thicknesses of the order of 10 nm, and well-isolated grains approaching 10 nm in size.⁵ Here, we describe films with oriented island-like FePt crystallites of the $L1_0$ -type structure prepared by growth of α -Fe particles on $\langle 100 \rangle$ oriented Pt "seed" particles followed by annealing to obtain the atomic ordering.

The sample preparation was performed using an electron-beam evaporation system. The pressure of the chamber was maintained better than 4×10^{-7} Pa prior to the deposition, and better than 4×10^{-5} Pa during the deposition. Pure Pt, Fe, and Al₂O₃ crystals were used as evaporation sources. Freshly cleaved NaCl (100) crystals as well as polished clean MgO (100) wafers were used as substrates. The choice of NaCl (100) crystals was to facilitate microstructural observation, although they are not stable in humid environment as compared with the MgO (100) wafers. The substrates were kept at approximately 400 °C during the deposition. A quartz thickness monitor was used to estimate the average thickness of the deposited layers. First, Pt was deposited at 0.1 nm/min on the substrate. Then, Fe was de-

posited at 0.4 nm/min onto the substrate with the Pt. In order to protect the iron film from oxidizing, a continuous cover layer of amorphous (a -)Al₂O₃ with a thickness greater than 5 nm was deposited further without breaking vacuum. The average thicknesses of all the Pt and all the Fe layers were set to be approximately 1.5 and 1.0 nm, respectively. To also obtain a film with only Pt particles, a part of the NaCl substrates was shielded from the Fe flux after the Pt deposition. Postannealing of the a -Al₂O₃/Fe/Pt films on the MgO and NaCl substrates was done at 600 °C for times ranging from 1 to 6 h in a vacuum better than 2×10^{-5} Pa. The NaCl substrates were immersed into distilled water to remove the a -Al₂O₃/Pt or a -Al₂O₃/Fe/Pt films, and the as-deposited or annealed films were mounted on copper microgrids for transmission electron microscopy (TEM) observations at 200 and 300 kV. *In situ* TEM observations, while annealing, were also made at 200 kV using a specimen heating stage. In-plane magnetization hysteresis loops of the as-deposited and annealed films on NaCl or MgO substrates were measured at room temperature with a superconducting quantum interference device magnetometer (SQUID).

TEM observation of the as-deposited a -Al₂O₃/Pt and a -Al₂O₃/Fe/Pt films revealed that the Pt crystals exhibit an island-like morphology and Fe particles were formed around the Pt particles. Figure 1 shows the TEM image (a) and selected area electron diffraction (SAED) pattern (b) of the as-deposited a -Al₂O₃/Pt film, and the SAED pattern of the unannealed a -Al₂O₃/Fe/Pt film (c). Some of the Pt crystals in Fig. 1(a) exhibit a well-defined morphology with facets; very similar to the morphology of Au particles in a -Al₂O₃/Au film prepared under similar experimental conditions.⁶ The diffraction spots in Fig. 1(b) were indexed as those of $\langle 100 \rangle$ oriented Pt crystals. From Fig. 1(c), it is

^{a)}Now located at the Data Storage Systems Center, Carnegie Mellon University; Electronic mail: bobian@ece.cmu.edu

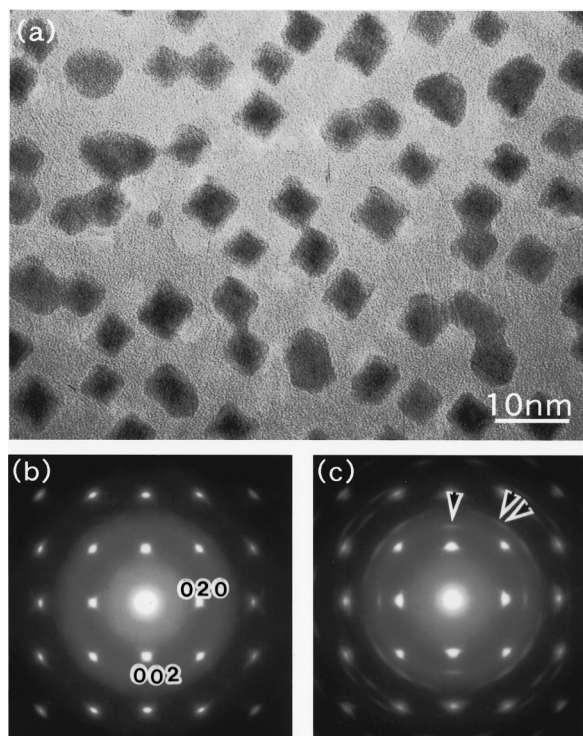


FIG. 1. TEM image (a) and SAED pattern (b) of the as-deposited $a\text{-Al}_2\text{O}_3/\text{Pt}$ film, and SAED pattern of the unannealed $a\text{-Al}_2\text{O}_3/\text{Fe/Pt}$ film (c). The bright spots in (b) correspond to $\langle 100 \rangle$ oriented fcc Pt crystals. The strong and weak reflections in (c) can be indexed as those of Pt and $\alpha\text{-Fe}$ crystals, respectively. The 002 and 112 reflections of $\alpha\text{-Fe}$ are marked by single and double arrows in (c), respectively.

seen that Fe deposition on the substrate with Pt crystals leads to the formation of $\alpha\text{-Fe}$.

No significant structural change was observed while the $a\text{-Al}_2\text{O}_3/\text{Fe/Pt}$ film was annealed below 450°C in the electron microscope. When the *in situ* annealing temperature reached 500°C , a gradual disappearance of the reflections from $\alpha\text{-Fe}$ was observed, and the appearance of the diffrac-

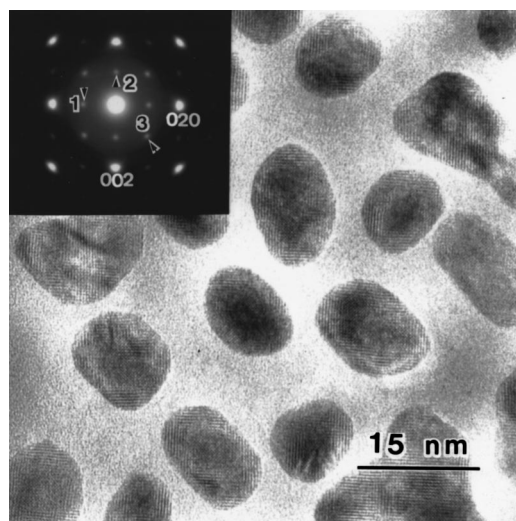


FIG. 2. TEM image and corresponding SAED pattern of the $a\text{-Al}_2\text{O}_3/\text{Fe/Pt}$ film annealed at 600°C for 6 h. The oriented crystals with the size of about 10 nm are well separated by the $a\text{-Al}_2\text{O}_3$. The superlattice reflections of 001 and 110 (marked as 1, 2, and 3) from three variants of $L1_0$ are observed, together with the 020 and 002 fundamental reflections. Any one of the three $\langle 100 \rangle$ axes of the fcc Pt parent phase can act as the tetragonal c axis of the $L1_0$ superstructure.

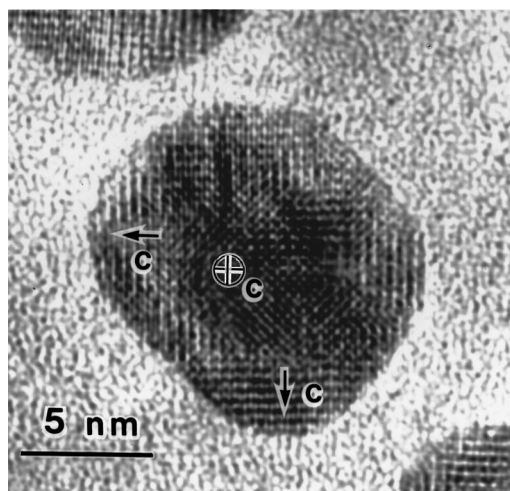


FIG. 3. HREM image of an ordered $L1_0$ FePt crystal in the $a\text{-Al}_2\text{O}_3/\text{Fe/Pt}$ film after 600°C annealing. The crystal consists of three components of the tetragonal phase. The c axis of the central region of the particle (marked as \oplus) was parallel to the electron beam and those of the other two variants in the outer regions of the nanocrystal (marked as \leftarrow and \downarrow) were in the horizontal plane.

tion pattern of the $\langle 100 \rangle$ oriented fcc (Fe–Pt) structure started. As the annealing was continued, superlattice diffraction spots began to appear and the intensity gradually increased. Figure 2 shows a typical TEM image and the corresponding SAED pattern of the $a\text{-Al}_2\text{O}_3/\text{Fe/Pt}$ film annealed at 600°C for 6 h. Uniformly dispersed isolated particles in $a\text{-Al}_2\text{O}_3$ can be seen. The average size of the particles in this film was estimated to be 12 nm. The average space between particles was approximately 4 nm, which was larger than that in the previous thin granular films discussed in the literature.² It has been reported that physical gaps of 2–5 nm appear to be sufficient to decouple the magnetic grains.⁷ The intergranular $a\text{-Al}_2\text{O}_3$ structure with an average thickness of about 4 nm should eliminate or significantly reduce intergrain exchange coupling, which is one of the main reasons for media noise.⁸ From the distance measurements of the diffraction spots in the SAED pattern, it was found that the superlattice spots correspond to three variants of the tetragonal $L1_0$ -type ordered FePt particles. Any one of the three $\langle 100 \rangle$ axes of the fcc Pt parent phase can correspond to the tetragonal c axis of the superstructure. Figure 3 shows a high-resolution electron microscopy (HREM) image of an ordered FePt crystal in the film annealed at 600°C . The image exhibits three structural domains corresponding to the variants of the tetragonal structure. The c axis of the central

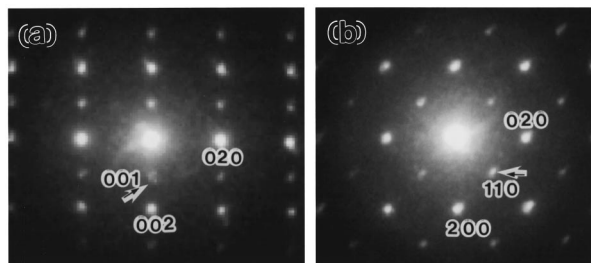


FIG. 4. NBD patterns obtained from different regions of an ordered FePt crystal by applying a beam probe of approximately 1 nm. The NBD patterns corresponded to local regions in the particle with the c axes perpendicular (a) and parallel (b) to the electron beam, respectively.

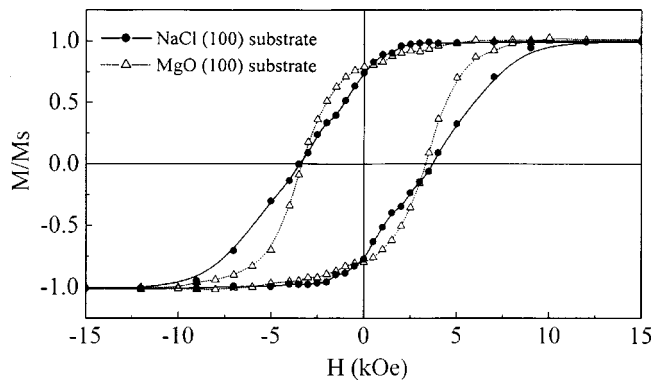


FIG. 5. In-plane hysteresis loops for the annealed (600 °C for 6 h) $a\text{-Al}_2\text{O}_3/\text{Fe}/\text{Pt}$ films on NaCl (100) and MgO (100) substrates. The magnetic coercivities for the annealed films on the NaCl (100) and MgO (100) substrates are 3.5 and 3.3 kOe, respectively.

region of the particle is parallel to the electron beam and that of the other two orthogonal variants, in the outer regions of the crystal, are in the horizontal plane. It is interesting that three-variant ordered crystalline domains of the tetragonal phase could coexist in such a small FePt crystal. Nanobeam electron diffraction (NBD) examination was also performed by focusing an electron nanoprobe on local regions of various FePt particles. The common existence of the three variants in the $L1_0$ particles was confirmed by the NBD examination. Figure 4 shows examples of NBD patterns obtained from different regions of a FePt nanocrystal by applying a beam probe of approximately 1 nm. Obviously, the NBD patterns corresponded to local regions with the c axes parallel and perpendicular to the electron beam, respectively.

The as-deposited $a\text{-Al}_2\text{O}_3/\text{Fe}/\text{Pt}$ films on both the NaCl and MgO substrates exhibited small magnetic coercivity (less than 40 Oe). However, the magnetic coercivity of the films was found to increase significantly after conversion to the $L1_0$ phase by annealing at 600 °C. In-plane hysteresis loops for the annealed (600 °C for 6 h) $a\text{-Al}_2\text{O}_3/\text{Fe}/\text{Pt}$ films on NaCl (100) and MgO (100) substrates are shown in Fig. 5. The magnetic coercivity and magnetic squareness for the annealed film on NaCl (100) was 3.5 kOe and 0.74, respectively. The magnetic coercivity for the annealed film on MgO (100) reached as high as 3.3 kOe with a squareness of 0.77. From the above similarity of the magnetic data for the films on the MgO and NaCl substrates, one is inclined to

believe that a similar microstructural change, upon annealing, occurs for the $a\text{-Al}_2\text{O}_3/\text{Fe}/\text{Pt}$ films on both substrates.

The tetragonal $L1_0$ FePt phase is characterized by a high uniaxial magnetocrystalline anisotropy with an “easy” c axis. The calculated magnetocrystalline anisotropy energy for the FePt ordered ($L1_0$) phase is about $1.6 \times 10^7 \text{ J/m}^3$.⁹ The ordered ($L1_0$) and oriented natures of the FePt crystals contribute to the high coercivity of the films. It is expected that the hard magnetic properties of the $L1_0$ FePt particles will be significantly improved if they are singly oriented with the tetragonal c axis all parallel or all perpendicular to the film plane. If the as-deposited $a\text{-Al}_2\text{O}_3/\text{Fe}/\text{Pt}$ films are annealed under a magnetic field, the FePt particles may form as a single variant. Our next step is to produce granular magnetic films with the above-oriented single-crystalline magnetic particles.

In summary, annealing of the $a\text{-Al}_2\text{O}_3/\text{Fe}(1 \text{ nm})/\text{Pt}(1.5 \text{ nm})$ film at temperatures higher than 500 °C leads to the formation of the ordered $L1_0$ FePt phase. Any one of the three $\langle 100 \rangle$ axes of the fcc Pt phase act as the tetragonal c axis of the $L1_0$ superstructure. Three-variant ordered domains of the tetragonal $L1_0$ phase can coexist in a single small 10 nm FePt crystal. The magnetic coercivities of the annealed (600 °C for 6 h) $a\text{-Al}_2\text{O}_3/\text{Fe}(1 \text{ nm})/\text{Pt}(1.5 \text{ nm})$ films on both the NaCl (100) and MgO (100) substrates are higher than 3.3 kOe. The present fabrication method may be useful for high-density recording media.

The authors wish to thank Professor David E. Laughlin and Dr. T. Ohkubo for their valuable discussions and help in this research. This study was supported by a Grant-in-Aid for Scientific Research from the Ministry of Education, Science and Culture, Japan.

- ¹D. N. Lambeth, E. M. T. Velu, G. H. Bellesis, L. L. Lee, and D. E. Laughlin, *J. Appl. Phys.* **79**, 4496 (1996).
- ²T. Hayashi, S. Hirono, M. Tomita, and S. Umemura, *Nature (London)* **381**, 772 (1996).
- ³K. R. Coffey, M. A. Parker, and J. K. Howard, *IEEE Trans. Magn.* **31**, 2737 (1995).
- ⁴B. R. Acharya, E. N. Abarra, G. N. Phillips, T. Suzuki, K. Adachi, N. Kitagaki, and M. Aihara, *IEEE Trans. Magn.* **34**, 1594 (1998).
- ⁵M. H. Kryder, *MRS Bull.* **21**, 17 (1996).
- ⁶B. Bian, Y. Hirotsu, and A. Makino, *Nanostruct. Mater.* **8**, 1057 (1997).
- ⁷T. Yogi and T. A. Nguyen, *IEEE Trans. Magn.* **29**, 307 (1993).
- ⁸T. Chen and T. Yamashita, *IEEE Trans. Magn.* **24**, 2700 (1988).
- ⁹A. Sakuma, *J. Phys. Soc. Jpn.* **63**, 3053 (1994).